

On Vehicle Placement to Intercept Moving Targets^{☆,☆☆}

Shaunak D. Bopardikar^{*.a}, Stephen L. Smith^b, Francesco Bullo^a

^aCenter for Control Dynamical Systems and Computation, University of California, Santa Barbara, CA 93106, USA

^bComputer Science and Artificial Intelligence Laboratory, Massachusetts Institute of Technology, Cambridge MA 02139, USA

Abstract

We address optimal placement of vehicles with simple motion, to intercept a mobile target that arrives stochastically on a line segment. The optimality of vehicle placement is measured through a cost function associated with intercepting the target. With a single vehicle, we assume that the target either moves with fixed speed and in a fixed direction or moves to maximize the vertical height or intercept time. We show that each of the corresponding cost functions is convex, has smooth gradient and has a unique minimizing location, and so the optimal vehicle placement is obtained by any standard gradient-based optimization technique. With multiple vehicles, we assume that the target moves with fixed speed and in fixed direction. We present a discrete time partitioning and gradient-based algorithm, and characterize conditions under which the algorithm asymptotically leads the vehicles to a set of critical configurations of the cost function.

Key words: Coverage control, Pursuit-evasion games, Optimization, Autonomous and Multi-agent systems.

1. Introduction

Vehicle placement to provide optimal coverage has received lot of recent attention due to potential applications in environmental monitoring, patrolling a piece of land between nations and even in popular games such as soccer. This work addresses vehicle placement to minimize a cost associated with intercepting a mobile target that appears randomly on a segment.

In static environments, vehicle placement problems are analogous to geometric location problems, wherein given a set of static points, the goal is to find supply locations that minimize a cost function of the distance from each point to its nearest supply location (cf. Megiddo and Supowit (1984) and Zemel (1984)). For a single vehicle, the average distance to a random point, generated according to a probability density function is given by the Weber or the continuous 1–median function, for which there exists a global minimizer as shown in Fekete et al. (2005), termed as the *median*. For multiple distinct vehicle locations, the

expected distance between a random point generated according to a probability density and one of the locations is known in literature as the continuous Weber or the continuous multi-median function, e.g., see Drezner (1995). For more than one location, the multi-median function is non-convex, and thus determining locations that minimize the multi-median function is hard in the general case. It is of interest to characterize the set of critical points of the multi-median function. Cortés et al. (2004) have characterized the set of critical points for the problem of deploying a group of robots in a region to optimize a multi-median cost function. Schwager et al. (2009) provide an adaptive control law to enable robots to approximate the density function from sensor measurements. Martínez and Bullo (2006) presented motion coordination algorithms to steer a mobile sensor network to an optimal placement. More recently, Kwok and Martínez (2010) presented a coverage algorithm for vehicles in a river environment.

In mobile target scenarios, the cost for the vehicle is a function of relative locations, speeds and motion constraints considered. For an adversarial target, the optimal vehicle motion is obtained by solving a min-max pursuit-evasion game, in which the target seeks to maximize while the vehicle seeks to minimize a certain cost function. The vehicle strategy is a version of the classic proportional navigation guidance law (cf. Guelman (1971)). With constraints such as a wall in the playing space or non-zero capture distance, strategies with optimal intercept time have been derived in Isaacs (1965) and in Pachter (1987).

We consider a line segment on which a mobile target appears via a known spatial probability density and one or multiple vehicles seek to intercept it. The goal is to determine vehicle placements that minimize a cost function associated with the target motion. This work is an exten-

[☆]This material is based upon work supported in part by ARO MURI Award W911NF-05-1-0219 and ONR Award N00014-07-1-0721 and by the Institute for Collaborative Biotechnologies through the grant DAAD19-03-D-0004 from the U.S. Army Research Office. The authors thank Prof. Jorge Cortés at the University of California, San Diego for insightful discussions leading to the proof of Lemma 3.3.

^{☆☆}A preliminary version of this work entitled “Vehicle Placement to Intercept Moving Targets” will be presented at the 2010 American Control Conference, Baltimore, MD, USA.

^{*}Corresponding author, Tel: +1-805-893-2801, Fax: +1-805-893-8651.

Email addresses: shaunak@engr.ucsb.edu (Shaunak D. Bopardikar), slsmith@mit.edu (Stephen L. Smith), bullo@engr.ucsb.edu (Francesco Bullo)

sion of Bopardikar et al. (2010), where we introduced the placement problem for target motion with fixed speed and in fixed direction, and for a uniform target arrival density. We address single and multiple vehicle scenarios. With a single vehicle, we consider a class of cost functions and establish properties such as convexity, smoothness and the existence and uniqueness of a globally minimizing vehicle location. We show that the cost functions associated with the target moving with fixed speed and in a fixed direction, and with the target seeking to maximize the distance from the segment, fall in the class of cost functions that we have analyzed. The cost function for target motion that maximizes the intercept time is shown to be proportional to the continuous 1–median function. With multiple vehicles and the target moving with fixed speed and in a fixed direction, we first provide an algorithm to partition the line segment among the vehicles and characterize its properties. With the expected intercept time as the cost function, we propose a Lloyd descent algorithm in which every vehicle computes its partition and moves along the gradient of the expected time computed over its partition. We characterize conditions under which the vehicles asymptotically reach a set of critical configurations.

This paper is organized as follows. The problem is formulated in Section 2. Single vehicle scenarios are addressed in Section 3. The multiple vehicle scenario is analyzed in Section 4.

2. Problem Statement

We consider vehicles with simple motion and speed upper bounded by unity. A target arrives at a random position $(x, 0)$ on the segment $G := [0, W] \times \{0\}$, termed the *generator*, via a specified probability density function $\phi : [0, W] \rightarrow \mathbb{R}_{\geq 0}$. We assume that the density function ϕ is bounded, i.e., there exists an $M > 0$ such that $\phi(x) \leq M, \forall x \in [0, W]$, and ϕ is positive on a set of positive measure. The target moves with bounded speed less than that of the vehicles, and is intercepted or captured if a vehicle and the target are at the same point. The goal is to determine vehicle placements that minimize a certain cost function based on the maneuvering abilities of the target. Specifically, we consider the following cases.

2.1. Single Vehicle Case

We determine a location $\mathbf{p} \in \mathbb{R} \times \mathbb{R}_{\geq 0}$ that minimizes $C_{\text{exp}} : \mathbb{R}^2 \rightarrow \mathbb{R}$ given by

$$C_{\text{exp}}(\mathbf{p}) := \int_0^W C(\mathbf{p}, x) \phi(x) dx, \quad (1)$$

where $C : \mathbb{R}^2 \rightarrow \mathbb{R}_{\geq 0}$ is an appropriately defined cost of the vehicle position \mathbf{p} . In what follows, we seek to minimize the following different cost functions.

(i) *Expected constrained travel time*: We assume that the target arriving at $(x, 0)$ translates in the positive Y -direction with speed $v < 1$. From Bopardikar et al. (2010),

the cost function C for this formulation is

$$T(\mathbf{p}, x) = \frac{\sqrt{(1-v^2)(X-x)^2 + Y^2}}{1-v^2} - \frac{vY}{1-v^2}, \quad (2)$$

which is the time taken for the vehicle to intercept the constrained target.

(ii) *Expected vertical height*: The cost function C for this formulation is the vertical height $H(\mathbf{p}, x)$ which the target seeks to maximize before being intercepted.

(iii) *Expected intercept time*: The cost function C for this formulation is the intercept time $\mathbf{Ti}(\mathbf{p}, x)$ which the target seeks to maximize.

Explicit formulae for the quantities H and \mathbf{Ti} are derived in Section 3.2, and are illustrated in Figure 1.

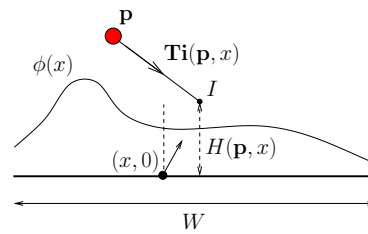


Figure 1: Intercepting a target that seeks to maximize either the vertical height H or the time \mathbf{Ti} until intercept.

2.2. Multiple Vehicles Case

We assume that the target translates in the positive Y -direction with speed $v < 1$. As shown in Figure 2, given $m \geq 2$ vehicles having complete communication, the goal is to determine vehicle locations $\mathbf{p}_i \in [0, W] \times \mathbb{R}_{\geq 0}$, for every $i \in \{1, \dots, m\}$, that minimize the expected constrained travel time given by

$$T_{\text{exp}}(\mathbf{p}_1, \dots, \mathbf{p}_m) := \int_0^W \min_{i \in \{1, \dots, m\}} T(\mathbf{p}_i, x) \phi(x) dx, \quad (3)$$

where $T(\mathbf{p}_i, x)$ is given by Eq. (2).

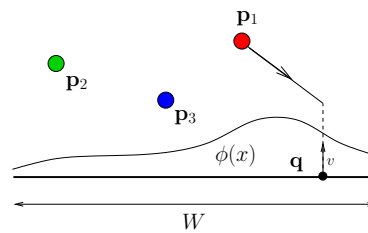


Figure 2: Intercepting a target having constrained motion.

3. Single Vehicle Scenarios

We first analyze a class of cost functions. This form will appear in two distinct scenarios, the expected constrained travel time and the expected vertical height.

3.1. A class of cost functions

We assume that the cost function is given by Eq. (1), where the function C has the form

$$C(X, Y, x) := a\sqrt{b(X-x)^2 + Y^2} - cY, \quad (4)$$

and a , b , and c are positive constants, with $a > c$.

The partial derivatives of $C_{\text{exp}}(X, Y)$ with respect to X and Y are given by

$$\frac{\partial C_{\text{exp}}}{\partial X} = ab \int_0^W \frac{(X-x)\phi(x)}{\sqrt{b(X-x)^2 + Y^2}} dx, \quad (5)$$

$$\frac{\partial C_{\text{exp}}}{\partial Y} = aY \int_0^W \frac{\phi(x)}{\sqrt{b(X-x)^2 + Y^2}} dx - c. \quad (6)$$

Lemma 3.1 (Convexity of expected cost) *The expected cost $C_{\text{exp}}(X, Y)$ is convex in X and Y over the domain $\mathbb{R} \times \mathbb{R}_{>0}$.*

The proof involves showing that the Hessian matrix of C with respect to X and Y is positive semi-definite. The complete proof is presented in ?.

Lemma 3.2 (Existence of Minima) *There exists a vehicle location $(X^*, Y^*) \in]0, W[\times \mathbb{R}_{>0}$ that minimizes C_{exp} .*

Proof: C_{exp} has continuous partial derivatives in the domain $]0, W[\times \mathbb{R}_{>0}$ (cf. Eq.s (5), (6)). We show that a minimizer cannot lie on the boundary of the region $[0, W] \times \mathbb{R}_{\geq 0}$. We begin by showing that Y^* exists and is finite. Taking the limit of $C_{\text{exp}}(X, Y)$ as $Y \rightarrow +\infty$,

$$\liminf_{Y \rightarrow +\infty} C_{\text{exp}}(X, Y) \geq \liminf_{Y \rightarrow +\infty} (a-c)Y \int_0^W \phi(x) dx = +\infty,$$

since by assumption, $a > c$. Thus, Y^* exists and is finite.

Finally, to show that a minimizer lies in $]0, W[\times \mathbb{R}_{>0}$, we need to prove two statements: (a) $Y^* \neq 0$, and (b) $X^* \in]0, W[$. To show (a), Eq. (6) along with the assumption $\phi(x) \leq M$, for every $x \in [0, W]$, yields

$$\begin{aligned} \frac{\partial C_{\text{exp}}}{\partial Y} &\leq MYa \int_0^W \frac{dx}{\sqrt{b(X-x)^2 + Y^2}} - c \\ &\leq \frac{MYa}{\sqrt{b}} (\log(W + \sqrt{W^2 + Y^2/b}) - \log(Y/\sqrt{b})) - c. \end{aligned}$$

Thus, $\limsup_{Y \rightarrow 0^+} \partial C_{\text{exp}}/\partial Y \leq -c$. Thus, for Y near zero the gradient of C_{exp} points in the negative Y -direction, implying that $Y^* \neq 0$.

To show (b), we first observe that for a given Y , in the limit as $X \rightarrow \pm\infty$, $C_{\text{exp}} \rightarrow +\infty$, and therefore X^* must be bounded. Finally, the claim follows since the partial derivative of C_{exp} with respect to X is strictly negative at $X = 0$ and is strictly positive at $X = W$.

These statements coupled with the convexity of C_{exp} with respect to X and Y imply the existence of a minimizer in the region $]0, W[\times \mathbb{R}_{>0}$. ■

Lemma 3.3 (Uniqueness) *There exists a unique vehicle location $(X^*, Y^*) \in]0, W[\times \mathbb{R}_{>0}$ that minimizes C_{exp} .*

Proof: Let there be two locations (X_1, Y_1) and (X_2, Y_2) that minimize the expected cost. From Lemma 3.1, since the expected cost C_{exp} is convex in X and Y , a convex combination of (X_1, Y_1) and (X_2, Y_2) also minimizes the expected time. Thus, the necessary conditions for minimum are satisfied by $(\bar{X}(\alpha), \bar{Y}(\alpha)) := (\alpha X_1 + (1-\alpha)X_2, \alpha Y_1 + (1-\alpha)Y_2)$, for every $\alpha \in [0, 1]$. Thus,

$$\begin{aligned} \int_0^W \frac{(\bar{X}(\alpha) - x)\phi(x)}{\sqrt{b\bar{X}(\alpha) - x)^2 + \bar{Y}(\alpha)^2}} dx &= 0, \\ \int_0^W \frac{\bar{Y}(\alpha)\phi(x)}{\sqrt{b(\bar{X}(\alpha) - x)^2 + \bar{Y}(\alpha)^2}} dx &= \frac{c}{a}. \end{aligned}$$

Since the above conditions hold for every $\alpha \in [0, 1]$, the partial derivatives of the above conditions evaluated at $\alpha = 0$, must equal zero. Thus, upon simplifying, we obtain,

$$\begin{aligned} \int_0^W \frac{(X_2 - x)Y_2(Y_1 - Y_2) - Y_2^2(X_1 - X_2)}{(b(X_2 - x)^2 + Y_2^2)^{3/2}} \phi(x) dx &= 0, \\ \int_0^W \frac{(X_2 - x)Y_2(X_1 - X_2) - (Y_1 - Y_2)(X_2 - x)^2}{(b(X_2 - x)^2 + Y_2^2)^{3/2}} \phi(x) dx &= 0, \end{aligned}$$

where $\phi(x)/(b(X_2 - x)^2 + Y_2^2)^{3/2} =: f(X_2, Y_2, x)$ is strictly positive for $Y_2 > 0$. Multiplying the first equation by $(X_1 - X_2)$, the second by $(Y_1 - Y_2)$, and adding the equations,

$$\int_0^W f(X_2, Y_2, x) (Y_2(X_1 - X_2) - (X_2 - x)(Y_1 - Y_2))^2 dx = 0.$$

Since $f(X_2, Y_2, x) \geq 0$, we must have $Y_2(X_1 - X_2) - (X_2 - x)(Y_1 - Y_2) = 0$, for every x at which $f(X_2, Y_2, x) > 0$, which is feasible only if $X_1 - X_2 = 0$ and $Y_1 - Y_2 = 0$. ■

We now present the main result for this section.

Theorem 3.4 (Minimizing expected cost) *From an initial location in $\mathbb{R} \times \mathbb{R}_{>0}$ and by using a gradient optimization technique, the vehicle reaches the unique point that minimizes the expected cost C_{exp} .*

Proof: The gradient of C_{exp} with respect to X and Y is a continuous function of X and Y in the region $\mathbb{R} \times \mathbb{R}_{>0}$. The function C_{exp} is convex in X and Y (cf. Lemma 3.1) and has a unique minimizer in $]0, W[\times \mathbb{R}_{>0}$ (cf. Lemmas 3.2 and 3.3). Thus, a gradient optimization technique (cf. Boyd and Vandenberghe (2004)) leads the vehicle to the unique global minimizer of C_{exp} . ■

Let $\mathcal{V} \subset [0, W]$, and choose $\phi(x)$ such that $\phi(x) = 0, \forall x \in [0, W] \setminus \mathcal{V}$. Then, Theorem 3.4 yields the following result.

Corollary 3.5 (Any subset of generator) *Let $\mathcal{V} \subset [0, W]$ have positive measure. Then, from an initial location in $[0, W] \times \mathbb{R}_{>0}$, and following gradient descent with \mathcal{V} as the region of integration, the vehicle remains inside $[0, W] \times \mathbb{R}_{>0}$ at all subsequent times.*

Theorem 3.4 answers the problem of minimizing the expected value of T , given by Eq. (2), with $a := 1/(1-v^2)$, $b := (1-v^2)$ and $c := v/(1-v^2)$, and $a > c$. In general, it is difficult to provide closed form expressions for the vehicle location that minimizes the expected time. A special case is described in Remark 3.6.

Remark 3.6 (Equal speeds) In this case, the optimal placement in the X variable is at the *centroid* of the distribution ϕ , with the optimal Y given by

$$X^* = \int_0^W \phi(x)x dx; Y^* = \sqrt{\int_0^W \phi(x)(X^* - x)^2 dx}. \quad \square$$

3.2. Optimal Placement for Adversarial Target

We consider two types of cost functions that the evader tries to maximize; vertical height and intercept time.

3.2.1. Minimizing the Expected Vertical Height

We first present the solution to the differential game with payoff equal to the vertical height. If the evader is slower than the pursuer, then the Appolonius circle is the boundary of the set of all points which the evader can reach without being captured. The following property is stated in Isaacs (1965).

Proposition 3.7 (Appolonius circle during pursuit)

If the pursuer and the evader both travel straight toward a point U on the Appolonius circle, then any new such circle, obtained from a pair of simultaneous intermediate positions of the pursuer and the evader, is tangent to the original circle at U , and is contained in the original circle.

The optimal pursuit strategy (cf. Isaacs (1965)) is to choose its velocity vector such that the line joining the pursuer and the evader remains parallel at all times, while reducing the distance. So for optimal placement, it suffices to determine the optimal evader strategy. Algorithm 1 summarizes our evader strategy, shown in Figure 3.

Algorithm 1: Move towards top-most

Assumes: Pursuer at (X, Y) . Evader at $(x, 0)$.

1: Compute center and radius of the Appolonius circle:

$$O := (O_x, O_y) = \left(\frac{x - v^2 X}{1 - v^2}, \frac{-v^2 Y}{1 - v^2} \right),$$

$$R := \frac{v}{1 - v^2} \sqrt{(X - x)^2 + Y^2}.$$

2: Move towards the point $(O_x, O_y + R)$ with speed v .

The following result is immediate from Proposition 3.7.

Lemma 3.8 (Move towards top-most is optimal) *The strategy move towards top-most is the evader's optimal*

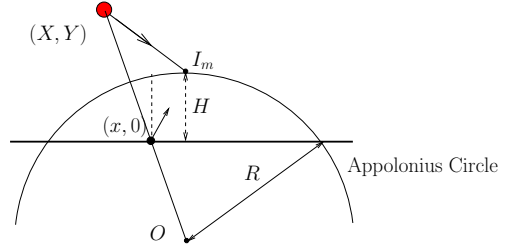


Figure 3: Move towards top-most strategy for the evader.

strategy and the resulting optimal vertical height of the intercept point is

$$H(X, Y, x) = \frac{v}{1 - v^2} \sqrt{(X - x)^2 + Y^2} - \frac{v^2 Y}{1 - v^2}.$$

Comparing the expression for H given by Lemma 3.8 with the definition of C in Eq. (4), we have $a := v/(1 - v^2)$, $b := 1$ and $c := v^2/(1 - v^2)$, and $a > c$ since $v < 1$. Thus, by applying Theorem 3.4, we obtain the following result.

Theorem 3.9 (Minimizing expected height) *From an initial location in $\mathbb{R} \times \mathbb{R}_{>0}$, by using a gradient optimization technique, the vehicle reaches the unique point that minimizes the expected height H_{exp} .*

3.2.2. Minimizing the Expected Intercept Time

In this formulation, we assume that the evader is constrained to remain above or on the X -axis. Thus, the underlying differential game in this set up is the classic *wall pursuit* game, proposed and solved in Isaacs (1965). We present the main result for completeness.

Lemma 3.10 (Wall Pursuit game) *The evader strategy that maximizes the intercept time is to move towards the furthest point of the Appolonius circle on the X -axis.*

This optimal evader strategy is illustrated in Figure 4.

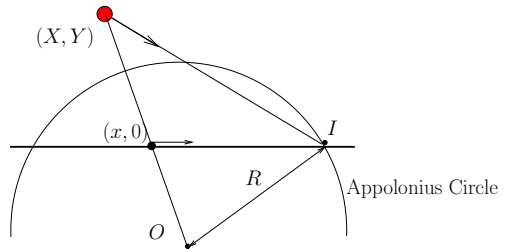


Figure 4: Illustrating Lemma 3.10.

Now, given a convex region $\mathcal{Q} \subset \mathbb{R}$ and a density function $\psi : \mathcal{Q} \rightarrow \mathbb{R}_{\geq 0}$, the *median* (cf. Fekete et al. (2005)) p_{med} is the unique global minimizer of

$$\int_{\mathcal{Q}} |p - z| \psi(z) dz.$$

We now present the main result of this section.

Theorem 3.11 (Optimal location is the Median) *The median point of the region $[0, W] \times \{0\}$ with the density function ϕ uniquely minimizes the expected intercept time.*

Proof: Using Lemma 3.10 and the Pythagoras theorem, the intercept time \mathbf{Ti} is given by

$$\mathbf{Ti}(X, Y, x) = \sqrt{R^2 - \left(\frac{vY}{1-v}\right)^2} + \left| \frac{x - vX}{1-v} - x \right|,$$

where R is the radius of the Apollonius circle drawn at the initial instant. Since pursuer placement on the X -axis results into decreasing the intercept time \mathbf{Ti} , we have

$$\mathbf{Ti}_{\text{exp}}(X) = \frac{v^2 + 3v}{1-v^2} \int_0^W |X - x| \phi(x) dx,$$

which is minimized uniquely by the median of the region $[0, W] \times \{0\}$ with the density function ϕ . \blacksquare

4. The Case of Multiple Vehicles

We now address the multi-vehicle placement problem.

4.1. Dominance Region Partition

We introduce a generator partitioning procedure by defining dominance regions between each pair of vehicles.

Definition 4.1 (Pairwise dominance region) *For $i, j \in \{1, \dots, m\}$, the pairwise dominance region $U_{ij} \subseteq [0, W]$ of \mathbf{p}_i with respect to \mathbf{p}_j is the set of target locations for which vehicle \mathbf{p}_i takes lesser time to intercept the target than \mathbf{p}_j :*

$$U_{ij} := \{x \in [0, W] \mid T(\mathbf{p}_i, x) \leq T(\mathbf{p}_j, x)\}.$$

In what follows, we describe a procedure to determine U_{ij} , which is summarized in Algorithm 2. Without loss of generality, assume that $X_i < X_j$. If $Y_i = Y_j$, i.e., the vehicles are at the same distance from the generator, then U_{ij} is the piece of G that lies in the half-plane that is formed by the perpendicular bisector of the segment joining \mathbf{p}_i and \mathbf{p}_j and which contains \mathbf{p}_i . Now if $Y_i < Y_j$, then we look for points $(x, 0)$ in G for which $T(\mathbf{p}_i, x) \leq T(\mathbf{p}_j, x)$. By setting $(1 - v^2) =: b$, Eq. (2) gives

$$\sqrt{b(X_i - x)^2 + Y_i^2} - vY_i \leq \sqrt{b(X_j - x)^2 + Y_j^2} - vY_j. \quad (7)$$

On simplifying, one can show that Eq. (7) is quadratic in x having real roots, which provides at most two points for the boundary between U_{ij} and U_{ji} . To determine the boundary points, consider the perpendicular bisector of the segment joining \mathbf{p}_i and \mathbf{p}_j , as shown in Figure 5. We look for points A_1 and A_2 on this bisector such that the distances of A_1 and A_2 from the real line is v times their respective distances from the vehicles. This gives rise to the following quadratic equation in the variable ℓ

$$4(\sin^2 \theta - v^2)\ell^2 + 4(Y_i + Y_j) \sin \theta \ell = -(Y_i + Y_j)^2 + v^2 \|\mathbf{p}_i - \mathbf{p}_j\|^2,$$

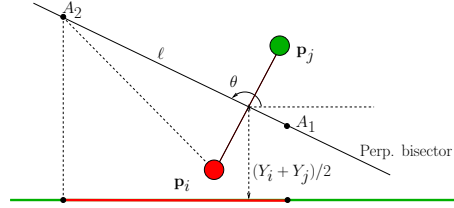


Figure 5: To determine pairwise dominance regions.

Algorithm 2: Pairwise Dominance Region

Assumes: Distinct $\mathbf{p}_i = (X_i, Y_i)$, $\mathbf{p}_j = (X_j, Y_j)$.

```

1: if  $Y_i = Y_j$ , then
2:    $U_{ij} := \begin{cases} [0, (X_i + X_j)/2], & \text{if } X_i < X_j \\ [(X_i + X_j)/2, W], & \text{if } X_i > X_j \end{cases}$ 
3: else
4:    $\theta := \arctan_2(Y_j - Y_i, X_j - X_i) + \pi/2$ 
5:    $\ell_{1,2} :=$  two roots of  $0 = 4(\sin^2(\theta) - v^2)\ell^2$ 
6:      $+ 4(Y_i + Y_j) \sin(\theta)\ell + (Y_i + Y_j)^2 - v^2 \|\mathbf{p}_i - \mathbf{p}_j\|^2$ 
7:    $y_{1,2} := (Y_i + Y_j)/2 + \sin(\theta)\ell_{1,2}$ 
8:   if  $y_1 > 0$  and  $y_2 > 0$  then
9:      $x_{1,2} := (X_i + X_j)/2 + \cos(\theta)\ell_{1,2}$ 
10:     $U_{ij} := \begin{cases} [0, W] \cap [x_1, x_2], & \text{if } Y_i < Y_j \\ [0, W] \setminus [x_1, x_2], & \text{if } Y_i \geq Y_j. \end{cases}$ 
11:  else
12:     $k :=$  index in  $\{1, 2\}$  for which  $y_k > 0$ 
13:     $x := (X_i + X_j)/2 + \ell_k \cos(\theta)$ 
14:     $U_{ij} := \begin{cases} [0, W] \cap [-\infty, x], & \text{if } X_i < X_j \\ [0, W] \cap [x, +\infty[, & \text{if } X_i \geq X_j \end{cases}$ 

```

where ℓ and $\theta := \arctan_2((Y_j - Y_i), (X_j - X_i)) + \pi/2$ are as shown in Figure 5. Let ℓ_1 and ℓ_2 be the roots of the above quadratic. Then the Y -coordinates of the candidate boundary points A_1 and A_2 are given by

$$[y_1, y_2]^T = [1, 1]^T (Y_i + Y_j)/2 + [\ell_1, \ell_2]^T \sin \theta.$$

Now, A_1 and A_2 are both boundary points if and only if both have positive Y -coordinates. It can be shown that there exists at least one among them which has positive Y -coordinate. There arise two cases:

(i) If there are two candidate points A_1 and A_2 (as in Figure 5), then we look at their corresponding X coordinates, (x_1, x_2) given by Step 7. For $(x, 0) \in G \cap [x_1, x_2] \times \{0\}$, we have $T(\mathbf{p}_i, x) \leq T(\mathbf{p}_j, x)$, and thus U_{ij} is $G \cap [x_1, x_2] \times \{0\}$.

(ii) If there is only one candidate point A_1 , then we look at its X coordinates, x_1 given by Step 9. By assumption $X_i < X_j$, and hence for $(x, 0) \in G \cap [-\infty, x_1] \times \{0\}$, we have $T(\mathbf{p}_i, x) \leq T(\mathbf{p}_j, x)$ and thus U_{ij} is $G \cap [-\infty, x_1] \times \{0\}$. Thus, we have established the following property.

Algorithm 3: Dominance region

Assumes: Distinct locations $\{\mathbf{p}_1, \dots, \mathbf{p}_m\}$.

- 1: **foreach** vehicle $j \in \{1, \dots, m\} \setminus \{i\}$, **do**
 - 2: Determine U_{ij} using Algorithm 2.
 - 3: $\mathcal{V}_i = \bigcap_{j=1, \dots, m, j \neq i} U_{ij}$.
-

Proposition 4.2 (Pairwise dominance region) *Given distinct locations $\mathbf{p}_i = (X_i, Y_i)$, $\mathbf{p}_j = (X_j, Y_j)$, if a target arrives at $(x, 0)$, where $x \in U_{ij}$ generated by Algorithm 2, then $T(\mathbf{p}_i, x) \leq T(\mathbf{p}_j, x)$.*

Similar to pairwise dominance regions, we introduce the concept of *dominance region* $\mathcal{V}_i \in \mathcal{P}([0, W])$ for the i th vehicle, for every $i \in \{1, \dots, m\}$, which is the set of X -coordinates of target locations for which \mathbf{p}_i takes the *minimum* time to intercept of all vehicles.

Assuming complete communication between vehicles, Algorithm 2 is extended to determine the dominance region for a vehicle by (i) determining pairwise dominance regions between vehicles and, (ii) taking intersection of all pairwise dominance regions, as presented in Algorithm 3.

The next result for Algorithm 3 follows due to disjoint interiors of dominance regions, and due to Proposition 4.2.

Proposition 4.3 (Optimality of dominance regions)

Given distinct vehicle positions and a target arrival,

- (i) *the dominance regions generated by Algorithm 3 form a partition of the generator.*
- (ii) *The time taken to reach the target is minimized by the vehicle whose dominance region contains the target arrival location.*

It is possible for the dominance region of a vehicle to be empty. For instance, when one of the vehicles is very far from the generating line (cf. first part of Figure 8). However, one condition under which every vehicle has a non-empty dominance region is when all vehicles have the same Y -coordinate. For a general set of locations, Figure 6 shows a dominance region partition with three vehicles.

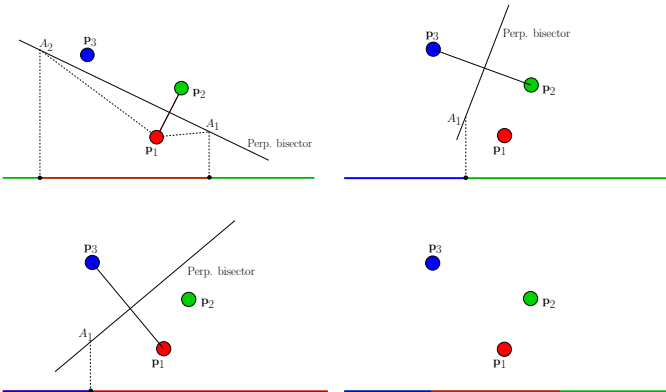


Figure 6: Dominance region partition induced by three vehicles.

Let $\mathcal{E} := [0, W] \times \mathbb{R}_{\geq 0}$, $\mathcal{P}([0, W])$ be the set of all subsets of $[0, W]$, $\mathcal{B}(r)$ be the closed ball of radius r around the origin and $+$ denote the Minkowski sum of two sets. The domain of a set-valued map $F : X \rightrightarrows Z$ is the set of all $\mathbf{q} \in X$ such that $F(\mathbf{q}) \neq \emptyset$. F is said to be upper (resp. lower) semi-continuous in its domain if, for every \mathbf{q} in its domain and for every $\epsilon > 0$, there exists a $\delta > 0$ such that for every $\mathbf{z} \in \mathbf{q} + \mathcal{B}(\delta)$, $F(\mathbf{z}) \subset F(\mathbf{q}) + \mathcal{B}(\epsilon)$ (resp. $F(\mathbf{q}) \subset F(\mathbf{z}) + \mathcal{B}(\epsilon)$). F is continuous in its domain if it is both upper and lower semi-continuous.

The pairwise dominance region between \mathbf{p}_i and \mathbf{p}_j is a set valued function $U_{ij} : \mathcal{E}^2 \setminus \mathcal{S}_{ij} \rightrightarrows \mathcal{P}([0, W])^2$, where $\mathcal{S}_{ij} \subset \mathcal{E}^2$ is the set of coincident locations for \mathbf{p}_i and \mathbf{p}_j . Similarly, the dominance region partition for vehicle i is a set-valued map $\mathcal{V}_i : \mathcal{E}^m \setminus \mathcal{S}_i \rightrightarrows \mathcal{P}([0, W])^{2(m-1)}$, where $\mathcal{S} \subset \mathcal{E}^m$ is the set of vehicle locations in which at least one other vehicle is coincident with \mathbf{p}_i .

Proposition 4.4 (Continuity of dominance regions) (i)

For every distinct i and j in the set $\{1, \dots, m\}$, the set valued map U_{ij} is continuous in $\mathcal{E}^2 \setminus \mathcal{S}_{ij}$.

- (ii) *For each vehicle $i \in \{1, \dots, m\}$, the set valued map \mathcal{V}_i is continuous on its domain.*

Proof: The roots of Eq. (7) which is a quadratic in x , vary continuously with \mathbf{p}_i and \mathbf{p}_j . Thus, the map $U_{i,j}$ is continuous in $\mathcal{E}^2 \setminus \mathcal{S}_{ij}$.

The domain of \mathcal{V}_i is contained in the domain of U_{ij} for every $j \neq i$. From part (i) of this Proposition, for every $j \neq i$, the set-valued map U_{ij} is upper semi-continuous in \mathcal{E}^2 . Thus, for every $j \neq i$, at every \mathbf{q} in the domain of \mathcal{V}_i and for every $\epsilon > 0$, there exist $\delta_{ij} > 0$ such that for every $\mathbf{z} \in \mathbf{q} + \mathcal{B}(\delta_{ij})$, $U_{ij}(\mathbf{z}) \subset U_{ij}(\mathbf{q}) + \mathcal{B}(\epsilon)$. Given an $\epsilon > 0$, by the choice of $\delta_i = \min\{\delta_{ij}, \forall j \neq i\}$, we obtain that for every $\mathbf{z} \in \mathbf{q} + \mathcal{B}(\delta_i)$, $\mathcal{V}_i(\mathbf{z}) \subset \mathcal{V}_i(\mathbf{q}) + \mathcal{B}(\epsilon)$. Thus \mathcal{V}_i is upper semi-continuous. Lower semi-continuity of \mathcal{V}_i is established similarly and the result follows. ■

4.2. Minimizing the Expected Constrained Travel Time

For distinct vehicle locations, Eq. (3) can be written as

$$T_{\text{exp}}(\mathbf{p}_1, \dots, \mathbf{p}_m) = \sum_{i=1}^m \int_{\mathcal{V}_i} T(\mathbf{p}_i, x) \phi(x) dx, \quad (8)$$

where \mathcal{V}_i is the dominance region of the i th vehicle. The gradient of T_{exp} is computed using the following formula.

Lemma 4.5 (Gradient computation) *For all vehicle configurations such that no two vehicles are at coincident locations, the gradient of the expected time with respect to vehicle location \mathbf{p}_i is*

$$\frac{\partial T_{\text{exp}}}{\partial \mathbf{p}_i} = \int_{\mathcal{V}_i} \frac{\partial T}{\partial \mathbf{p}_i}(\mathbf{p}_i, x) \phi(x) dx.$$

Akin to similar results in Cortés et al. (2004, 2005); Bullo et al. (2009), the proof involves writing the gradient as a sum of two contributing terms. The first is the final expression, while the second is a number of boundary terms

Algorithm 4: Lloyd descent for vehicle i

Assumes: Distinct locations $\{\mathbf{p}_1, \dots, \mathbf{p}_m\} \in \mathcal{E}^m$

```

1: foreach time  $t \in \mathbb{N}$  do
2:   Compute  $\mathcal{V}_i(t)$  by Algorithm 3 as a function of
    $\{\mathbf{p}_1(t), \dots, \mathbf{p}_m(t)\}$ 
3:   if  $\mathcal{V}_i(t)$  is empty, then
4:     Move in unit time to  $(X_i, Y_i - \min\{1, Y_i\})$ 
5:   else
6:     For  $\tau \in [t, t + 1]$ , move according to
      $\dot{\mathbf{p}}_i(\tau) = -\text{sat} \left( \int_{\mathcal{V}_i(t)} \frac{\partial}{\partial \mathbf{p}_i} T(\mathbf{p}_i(\tau), x) \phi(x) dx \right)$ 

```

which cancel out due to continuity of T at the boundaries of dominance regions. The complete proof is presented in ?.

For $\mathbf{z} \in \mathbb{R}^2$, define the function $\text{sat} : \mathbb{R}^2 \rightarrow \mathbb{R}^2$ denote the saturation function, i.e., if $\|\mathbf{z}\| \leq 1$, then $\text{sat}(\mathbf{z}) = \mathbf{z}$; otherwise, $\text{sat}(\mathbf{z}) = \mathbf{z}/\|\mathbf{z}\|$. Inspired by the established Lloyd algorithm (cf. Bullo et al. (2009)), we present a discrete-time descent approach in Algorithm 4.

We define the following vehicle configuration.

Definition 4.6 (Critical configuration) *A set of locations $\{\mathbf{p}_1, \dots, \mathbf{p}_m\}$ is a critical dominance region configuration if, for all $i \in \{1, \dots, m\}$,*

$$\mathbf{p}_i = \operatorname{argmin}_{\mathbf{z} \in \mathcal{E}} \int_{\mathcal{V}_i} T(\mathbf{z}, x) \phi(x) dx,$$

where $\{\mathcal{V}_1, \dots, \mathcal{V}_m\}$ is the dominance region partition induced by $\{\mathbf{p}_1, \dots, \mathbf{p}_m\}$.

We now state the main result of this section.

Theorem 4.7 (Convergence of Lloyd descent) *Let $\gamma : \mathbb{N} \rightarrow \mathbb{R}^{2m}$ be the evolution of the m vehicles according to Algorithm 4 and assume that no two vehicle locations become coincident in finite time or asymptotically. The following statements hold:*

- (i) *the expected travel time $t \mapsto T_{\text{exp}}(\gamma(t))$ is a non-increasing function of time;*
- (ii) *if the dominance region \mathcal{V}_i of any vehicle i is empty at some time, then \mathcal{V}_i will be non-empty within a finite time; and*
- (iii) *if there exists a time t such that every dominance region is non-empty for all times subsequent to t , then the vehicle locations converge to the set of critical dominance region configurations.*

Proof: We begin by showing statement (i). In every iteration of Algorithm 4, step 2: does not increase the expected time T_{exp} due to the optimality of the dominance region partition, by Proposition 4.3. Step 4: does not change the T_{exp} as the associated dominance region is empty. Finally, step 6: does not increase T_{exp} as the vehicle

is moving along the gradient descent flow of T_{exp} . Thus, the expected time is non-increasing under Algorithm 4.

Statement (ii) follows from the fact that whenever $\mathcal{V}_i = \emptyset$ for vehicle i , due to step 4:, vehicle i reaches the generator after finite time and therefore has a non-empty \mathcal{V}_i .

For non-empty \mathcal{V}_i , let $\mathcal{A} : \mathcal{X} \times \mathcal{P}([0, W]) \rightarrow \mathcal{X}$, be the flow map of the differential equation at step 6: from time t to time $t+1$. For statement (iii), consider the discrete-time dynamical system given by the tuple $(\mathcal{X}, \mathcal{X}_0, \mathcal{A})$, where $\mathcal{X} = \mathcal{E}^m$ and $\mathcal{X}_0 \in \mathcal{E}^m$ is the set of initial vehicle positions.

We now apply the discrete-time LaSalle Invariance Principle (Theorem 1.19 in Bullo et al. (2009)), for which we verify the four assumptions as follows.

1. Existence of a positively invariant set: At every iteration of step 6:, each vehicle follows saturated gradient descent of a cost function belonging to the class of Eq. (4) over its dominance region fixed for the iteration. By Corollary 3.5, each vehicle remains in \mathcal{E} throughout the iteration, and therefore at all times. Thus, the set \mathcal{E}^m is positively invariant for the system $(\mathcal{X}, \mathcal{X}_0, \mathcal{A})$.

2. Existence of a non-increasing function along \mathcal{A} : T_{exp} is non-increasing along \mathcal{A} , by statement (i) of this theorem.

3. Boundedness of all evolutions of $(\mathcal{X}, \mathcal{X}_0, \mathcal{A})$: Since gradient descent keeps the X coordinates bounded in $[0, W]$, it remains to show that the Y -coordinates of all vehicles remain bounded. Let us suppose the contrary. Then, there are two cases: (a) at least one vehicle has its location bounded and at least one other vehicle, say vehicle k moves so that Y_k grows unbounded; or (b) all of the vehicles move so that their Y -coordinates grow unbounded. In case (a), after finite time, the dominance region \mathcal{V}_k becomes empty, thus contradicting the assumption of statement (iii) of this theorem. If case (b) occurs, then T_{exp} grows unbounded, thus contradicting statement (i) of this theorem. Thus, all evolutions of $(\mathcal{X}, \mathcal{X}_0, \mathcal{A})$ are bounded.

4. Continuity of T_{exp} and \mathcal{A} : Continuity of T_{exp} follows from Eq.s (2) and (8). To verify continuity of \mathcal{A} , note that whenever \mathcal{V}_i is non-empty, by Proposition 4.4, \mathcal{V}_i is continuous with respect to vehicle locations. Thus, as long as \mathcal{V}_i is non-empty, \mathcal{A} is continuous as the integrand is continuous with respect to vehicle locations, and so is the region of integration \mathcal{V}_i .

By LaSalle Invariance Principle, the evolutions of $(\mathcal{X}, \mathcal{X}_0, \mathcal{A})$ converge to a set of the form $T_{\text{exp}}^{-1}(\kappa) \cap \mathcal{M}$, where κ is a real constant and \mathcal{M} is the largest positively invariant set in $\{x \in \mathcal{X} \mid T_{\text{exp}}(\mathcal{A}(x)) = T_{\text{exp}}(x)\}$. Since T_{exp} remains constant under action of \mathcal{A} for the set of critical dominance region configurations, it is contained in a set of the form $T_{\text{exp}}^{-1}(\kappa) \cap \mathcal{M}$. If a set of vehicle positions is not critical, then T_{exp} strictly decreases under the action \mathcal{A} , and therefore the set of vehicle positions is not contained in a set of $T_{\text{exp}}^{-1}(\kappa) \cap \mathcal{M}$. Thus, the vehicle locations converge to the set of critical dominance region configurations. ■

The next result gives a simple condition to identify an unstable critical dominance region configuration, which is an unstable equilibrium of Algorithm 4.

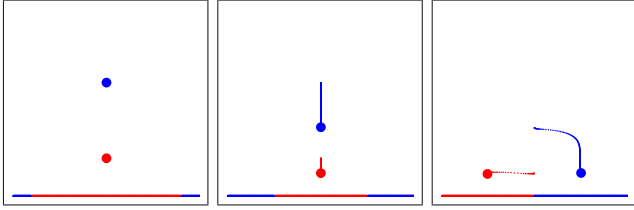


Figure 7: Algorithm 4 for uniform arrival density. The vehicles first tend to an critical dominance region configuration (center figure). A perturbation to their positions makes them move to a stable configuration (third figure).

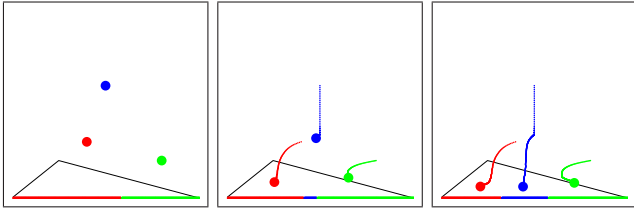


Figure 8: Algorithm 4 for non-uniform arrival density (black line). Initially, the blue vehicle has no dominance region. The vehicles tend to a stable configuration.

Lemma 4.8 (Disconnected partitions are unstable)
A critical dominance region configuration is unstable if some vehicle has disconnected dominance region partition.

The proof involves perturbing the position of a vehicle that has a disconnected dominance region in a critical dominance region configuration, and then showing that the resulting gradient in the X direction for that vehicle takes the vehicle away from the equilibrium configuration. The complete proof is presented in ?.

4.3. Simulations

We now present some simulations of Algorithm 4.

[Examples of critical locations] We consider two vehicles, and a uniform probability density of target arrival, i.e., $\phi(x) = 1/W$. From initial locations such as in the left-most of Figure 7 wherein both vehicles having the same X -coordinate of $W/2$, but different Y -coordinates, the vehicles asymptotically approach a set of locations shown in the center figure. However, a small perturbation to the positions leads the vehicles to positions in the rightmost figure. From most initial conditions, the vehicles converged to a critical configuration as in the rightmost figure.

[Non-uniform probability distribution] We consider three vehicles and the arrival probability density function,

$$\phi(x) = \begin{cases} 8x/W^2, & \text{if } x \in [0, W/4], \\ 2/W - 8(x - W/4)/(3W^2), & \text{if } x \in]W/4, W]. \end{cases}$$

From most initial conditions, the vehicles converged to a critical configuration as in right-most part of Figure 8.

5. Conclusions and Future Directions

We addressed the problem of optimally placing vehicles having simple motion in order to intercept a mobile

target that arrives stochastically on a line segment. For a single vehicle, we determined unique optimal placements when target motion was either constrained, i.e., with fixed speed and direction, or adversarial. For the multiple vehicle scenario and with constrained motion targets, we characterized conditions under which a partition and gradient based algorithm that takes the vehicles asymptotically to a set of critical locations of the cost function.

A natural future direction is to consider adversarial targets in the multiple vehicles scenario. Another direction is to consider stochasticity in the motion of the target.

References

- Bopardikar, S. D., Smith, S. L., Bullo, F., Mar. 2010a. On vehicle placement to intercept moving targets. Available at <http://arxiv.org/abs/1003.1423>.
- Bopardikar, S. D., Smith, S. L., Bullo, F., Hespanha, J. P., Jan. 2010b. Dynamic vehicle routing for translating demands: Stability analysis and receding-horizon policies. IEEE Transactions on Automatic Control (Submitted, Mar 2009) to appear.
- Boyd, S., Vandenberghe, L., 2004. Convex Optimization. Cambridge University Press.
- Bullo, F., Cortés, J., Martínez, S., 2009. Distributed Control of Robotic Networks. Applied Mathematics Series. Princeton University Press, available at <http://www.coordinationbook.info>.
- Cortés, J., Martínez, S., Bullo, F., 2005. Spatially-distributed coverage optimization and control with limited-range interactions. ESAIM: Control, Optimisation & Calculus of Variations 11, 691–719.
- Cortés, J., Martínez, S., Karatas, T., Bullo, F., 2004. Coverage control for mobile sensing networks. IEEE Transactions on Robotics and Automation 20 (2), 243–255.
- Drezner, Z. (Ed.), 1995. Facility Location: A Survey of Applications and Methods. Series in Operations Research. Springer.
- Fekete, S. P., Mitchell, J. S. B., Beurer, K., 2005. On the continuous Fermat–Weber problem. Operations Research 53 (1), 61 – 76.
- Guelman, M., 1971. A qualitative study of proportional navigation. IEEE Transactions on Aerospace and Electronic Systems 7 (4), 637–643.
- Isaacs, R., 1965. Differential Games. Wiley.
- Kwok, A., Martínez, S., 2010. A coverage algorithm for drifters in a river environment. In: American Control Conference. Baltimore, MD, to appear.
- Martínez, S., Bullo, F., 2006. Optimal sensor placement and motion coordination for target tracking. Automatica 42 (4), 661–668.
- Megiddo, N., Supowit, K. J., 1984. On the complexity of some common geometric location problems. SIAM Journal on Computing 13 (1), 182–196.
- Pachter, M., 1987. Simple motion pursuit-evasion in the half-plane. Computers and Mathematics with Applications 13 (1-3), 69–82.
- Schwager, M., Rus, D., Slotine, J. J., 2009. Decentralized, adaptive coverage control for networked robots. International Journal of Robotics Research 28 (3), 357–375.
- Zemel, E., 1984. Probabilistic analysis of geometric location problems. SIAM Journal on Algebraic and Discrete Methods 6 (2), 189–200.